EXPERIMENTAL and MOLECULAR MEDICINE, Vol. 41, No. 3, 151-160, March 2009

# Inhibition of cell proliferation by a resveratrol analog in human pancreatic and breast cancer cells

**Young Bin Hong[1]*, Hyo Jin Kang[1]*, Hee Jeong Kim[1], Eliot M. Rosen[1,2,3], Sivanesan Dakshanamurthy[1,4], Riccardo Rondanin[5], Riccardo Baruchello[5], Giuseppina Grisolia[5], Simoni Daniele[5], and Insoo Bae[1,2,6]**

[1]Department of Oncology
[2]Department of Radiation Medicine
[3]Department of Biochemistry and Molecular and Cellular Biology
[4]Drug Discovery Program
Lombardi Comprehensive Cancer Center
Georgetown University, 3970 Reservoir Road, NW
Washington DC, 20057-1469, USA
[5]Dipartimento di Scienze Farmaceutiche
Via Fossato di Mortara 17-19
Università di Ferrara, 44100 Ferrara, Italy
[6]Corresponding author: Tel, 1-202-687-5267;
Fax, 1-202-687-2847; E-mail, ib42@georgetown.edu
*These authors contributed equally to this work.
DOI 10.3858/emm.2009.41.3.018

Accepted 6 November 2008

Abbreviation: 11b, *cis*-3,4',5-trimethoxy-3'-hydroxystilbene

## Abstract

**Resveratrol has been reported to possess cancer preventive properties. In this study, we analyzed anti-tumor activity of a newly synthesized resveratrol analog, *cis*-3,4',5-trimethoxy-3'-hydroxystilbene (hereafter called 11b) towards breast and pancreatic cancer cell lines. 11b treatments reduced the proliferation of human pancreatic and breast cancer cells, arrested cells in the G2/M phase, and increased the percentage of cells in the subG1/G0 fraction. The 11b treatments also increased the total levels of mitotic checkpoint proteins such as BubR1, Aurora B, Cyclin B, and phosphorylated histone H3. Mechanistically, 11b blocks microtubule polymerization *in vitro* and it disturbed microtubule networks in both pancreatic and breast cancer cell lines. Computational modeling of the 11b-tubulin interaction indicates that the dimethoxyphenyl group of 11b can bind to the colchicine binding site of tubulin. Our studies show that the 11b treatment effects occur at lower concentrations than similar effects associated with resveratrol treatments and that microtubules may be the primary target for the observed effects of 11b. These studies suggest that 11b should be further examined as a potentially potent clinical chemotherapeutic agent for treating pancreatic and breast cancer patients.**

**Keywords:** antineoplastic agents, phytogenic; breast neoplasms; cell cycle; *cis*-3,4',5-trimethoxy-3'-hydroxystilbene; pancreatic neoplasms; resveratrol; tubulin

## Introduction

Numerous agents have been clinically tested as potential treatments for pancreatic cancer, one of the most life-threatening neoplasms. Due to late diagnosis and poorly understood carcinogenic mechanisms, adequate treatments for pancreatic cancer are not yet available (Lockhart *et al*., 2005; Jimeno and Hidalgo, 2006; Kim and Saif, 2007). Pancreatic cancer is also highly resistant to many currently available chemotherapies and to radiotherapy (Lockhart *et al*., 2005). In addition, although some neoadjuvant therapies have been tried in pancreatic cancer patients; for example, combining conventional external beam radiation with various combinations of anti-tumor drugs (e.g., 5-fluorouracil, gemcitabine, and paclitaxel) (Ishii *et al*., 1997; Epelbaum *et al*., 2002; Rich *et al*., 2004), no significant improvement in long-term survival has been observed (Kim and Saif, 2007).

In breast cancer, there are several options for neoadjuvant chemotherapy, even for locally advanced invasive stage tumors. Radiotherapy and some combinations of bevacizumab, docetaxel, doxorubicin, and cyclophosphamide have shown good efficacy (Buzdar, 2007). However, since individual breast cancers are themselves heterogeneous and since some portion of many individual breast tumors can be resistant to existing anti-tumor agents, there is no current "gold standard" treatment (Buzdar, 2007). Thus, additional therapeutic regimens need to be examined, and new patient-specific drugs need to be developed.

Resveratrol, *trans*-3,5,4'-trihydroxy-*trans*-stilbene, is a natural polyphenol with potent cancer preventive properties (Jang *et al*., 1997). It can modulate multiple cellular processes, including apoptosis,

cell cycle progression, inflammation, and angiogenesis (Athar *et al*., 2007). Resveratrol has some structural similarities to diethylstilbene, a synthetic estrogen. Recent studies showed that resveratrol can modulate cell signaling in metastatic breast cancer cells through the estrogen receptor (Le Corre *et al*., 2005; Azios *et al*., 2007). In addition, resveratrol treatments reduced metastasis in a HER2 transgenic mammary tumor mouse model (Provinciali *et al*., 2005). Resveratrol also inhibited proliferation in two human pancreatic cancer cell lines, PANC-1 and AsPC-1, in a dose and time dependent manner (Ding and Adrian, 2002). However, resveratrol does not always kill tumor cells ; for example, it failed to significantly reduce the size of *N*-nitrosobis (2-oxopropyl) amine induced tumors or block tumor formation in a hamster pancreatic carcinogenesis model (Kuroiwa *et al*., 2006). However, *cis*-3,4',5-trimethox-3'-hydroxystilbene (11b), a synthetic analog of resveratrol, showed greater anti-proliferative and pro-apoptotic activity than resveratrol in HL60 promyelocytic leukemia cell culture experiments (Roberti *et al*., 2003). Therefore, we determined whether 11b might be potentially useful for preventing and/or treating human pancreatic and breast cancers. In this study, we characterized the anti-proliferation activities of 11b on pancreatic and breast cancer cell lines and determined whether these effects are associated with the effects of 11b on microtubule dynamics (i.e., polymerization or depolymerization).

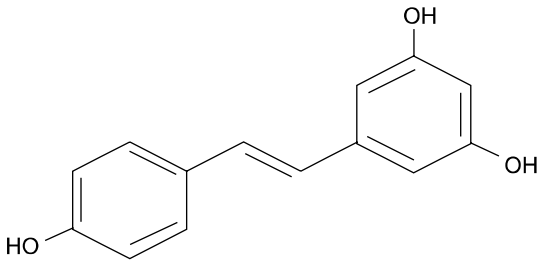


*trans*-3, 4', 5-trihydroxystilbene
(resveratrol)

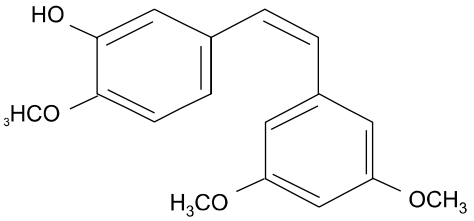


*cis*-3, 4', 5-trimethoxyl-3'-hydroxystilbene
(11b)

**Figure 1.** Structures of *trans*-resveratrol and 11b. 11b is a chemically synthesized resveratrol analog, in which substituents are introduced at positions 3, 4' and 5 with a methoxyl functional group.

## Results

### Structure of 11b

A resveratrol analog, 11b, was synthesized as we previously described (Roberti *et al*., 2003). 11b is a *cis*-stilbene with three $OCH_3$ groups at positions 3, 4' and 5 and one OH group at the 3' position, while resveratrol is a *trans*-stilbene with three OH group at positions 3, 4' and 5 (Figure 1).

### Effects of 11b on the viability of pancreatic and breast cancer cell

Three human pancreatic cell lines (PANC-1, AsPC-1, Colo-357) were exposed to different dose of resveratrol and 11b for 24 h. Resveratrol had relatively small effects on the viability, of PANC-1 cells (83% survival) and AsPC-1 cells (78%), even at 50 μM, the highest dose (Figure 2A) but had somewhat larger effects on Colo-357 viability (53% in 50 μM, $P < 0.001$). The viabilities of all three cell lines were significantly less when treated with 11b than when treated with the same concentrations of resveratrol and were dose dependent. For example, 1 μM of 11b reduced the viability of PANC-1 and Colo-357 to 57% and 63%, respectively and 50 μM of 11b reduced the viability of PANC-1, AsPC-1, and Colo-357 to 8%, 23%, and 7%, respectively. Survival of breast cancer cells (MCF-7 and MDA-MB-231) was also more significantly affected by 11b than by resveratrol (Figure 2B). Thus, 1 μM of 11b reduced the viability of MCF-7 and MDA-MB-231 cell to 43% and 57%, respectively, whereas incubation with 1 μM resveratrol did not detectably affect the viability of either MCF-7 (99%) or MDA-MB-231 (102%) cells.

### Effect of 11b on cell cycle progression

In order to assess the effect of 11b on cell cycle progression, we performed FACS analysis of cells after propidium iodide (PI) staining of cellular DNA. The cell cycle profiles of MDA-MB-231 (Figure 3A) and PANC-1 (Figure 3C) changed significantly after incubation with 10 μM of 11b for 24 h. In the diploid populations, the proportion of cells in the

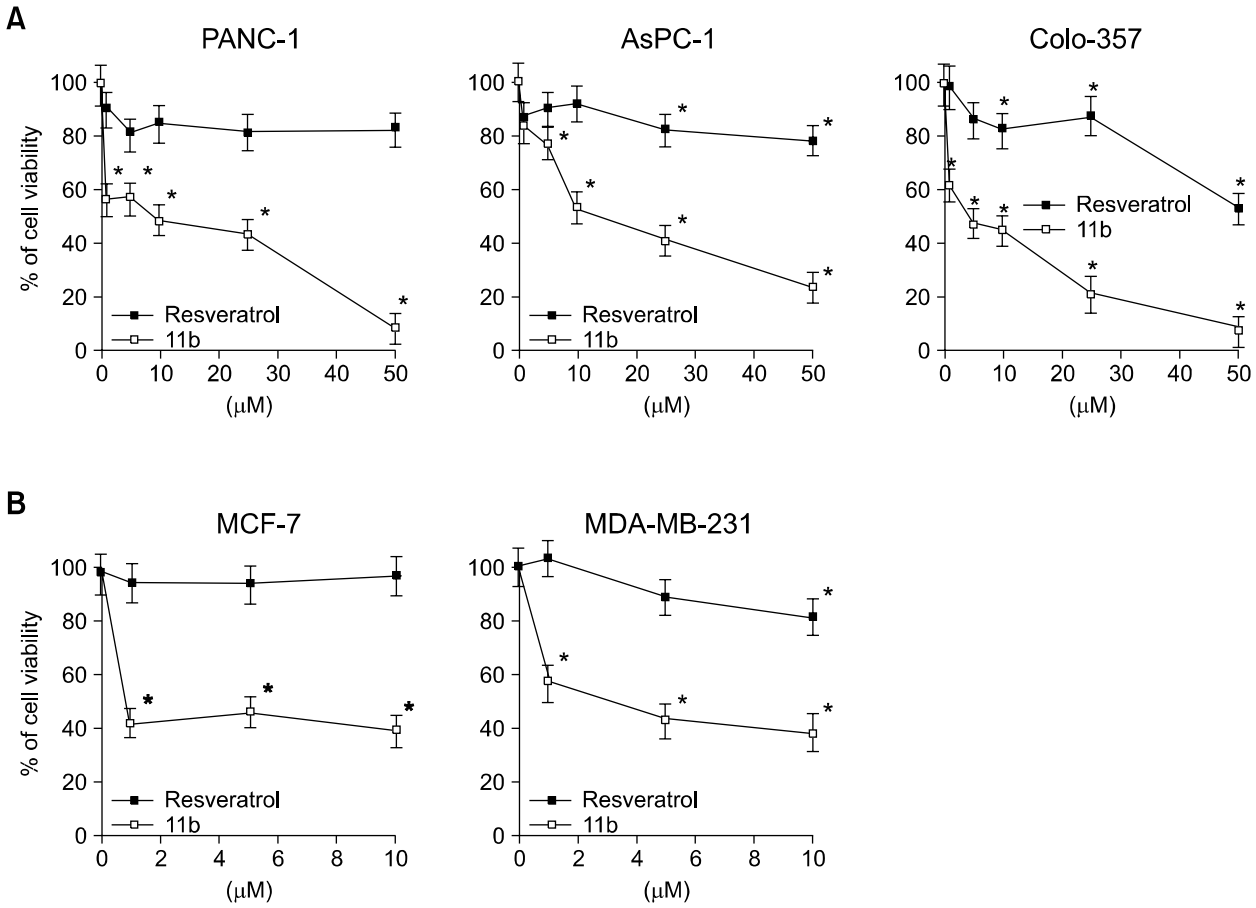


**Figure 2.** Effects of resveratrol and 11b on the survival of human pancreatic and breast cancer cells. (A) The viability of pancreatic cancer cell lines, PANC-1, AsPC-1, and Colo-357, was measured after 24 h treatments with 0, 1, 5, 10, 25, and 50 μM resveratrol or 11b. (B) The viability of breast cancer cell lines, MCF-7 and MDA-MB-231, was measured after 24 h treatments with 0, 1, 5, and 10 μM of resveratrol or 11b. The data is representative of three independent experiments. The two-tailed Student *t* test was used for statistical analysis and the symbol (*$P < 0.001$) in the figure indicates statistically significant differences from cells treated with the same concentrations of resveratrol.

G2/M DNA population increased from 11% to 98% in MDA-MB-231 (Figure 3B), and from 10% to 88% in PANC-1 (Figure 3D). On the other hand, the G1 phase decreased from 63% to 2% in MDA-MB-231 and from 56% to 12% in PANC-1 cells. There were no S phase cells observed after treating either cell line with 11b for 24 h. The sub-G0/G1 fraction increased 40.7-fold in MDA-MB-231 cells (Figure 3A) and 7.2-fold in PANC-1 cells (Figure 3C) after treatments with 10 μM 11b for 24 h.

### Elevation of mitotic checkpoint proteins expression

In order to test whether these 11b treatment effects were associated with mitotic cell cycle arrest, we looked for changes in the mobility of several mitotic checkpoint proteins by standard Western blot analysis. The mobility of BubR1 shifted in 11b-treated MDA-MB-231 cells while the mobility of about half of the BubR1 in PANC-1 cells had shifted following treatments with 5 μM 11b (Figure 4). Incubation of the cell lysates with lambda phosphatase before electrophoresis completely eliminated these mobility shifts, suggesting that a significant fraction of the total BubR1 protein is phosphorylated in 11b treated cells. This finding suggests that the 11b treatments are activating at least one mitotic checkpoint (Chen, 2002). We found that histone H3 was also phosphorylated by these 11b treatments (Figure 4). Phosphorylation of histone H3 is required for proper sister chromatid segregation (Wei *et al*., 1999). The amounts of the Aurora kinase, a mitotic spindle checkpoint kinase (Adams *et al*., 2001) that is important during the mitotic-phase phosphorylation of histone H3 at Ser-10 (Ota *et al*., 2002) were elevated in these 11b treated cells (Figure 4). In addition, the 11b treatments also significantly increased Cyclin B protein levels in both cell lines (Figure 4). Cyclin B is a key regulator of the cell cycle that controls the G2/M

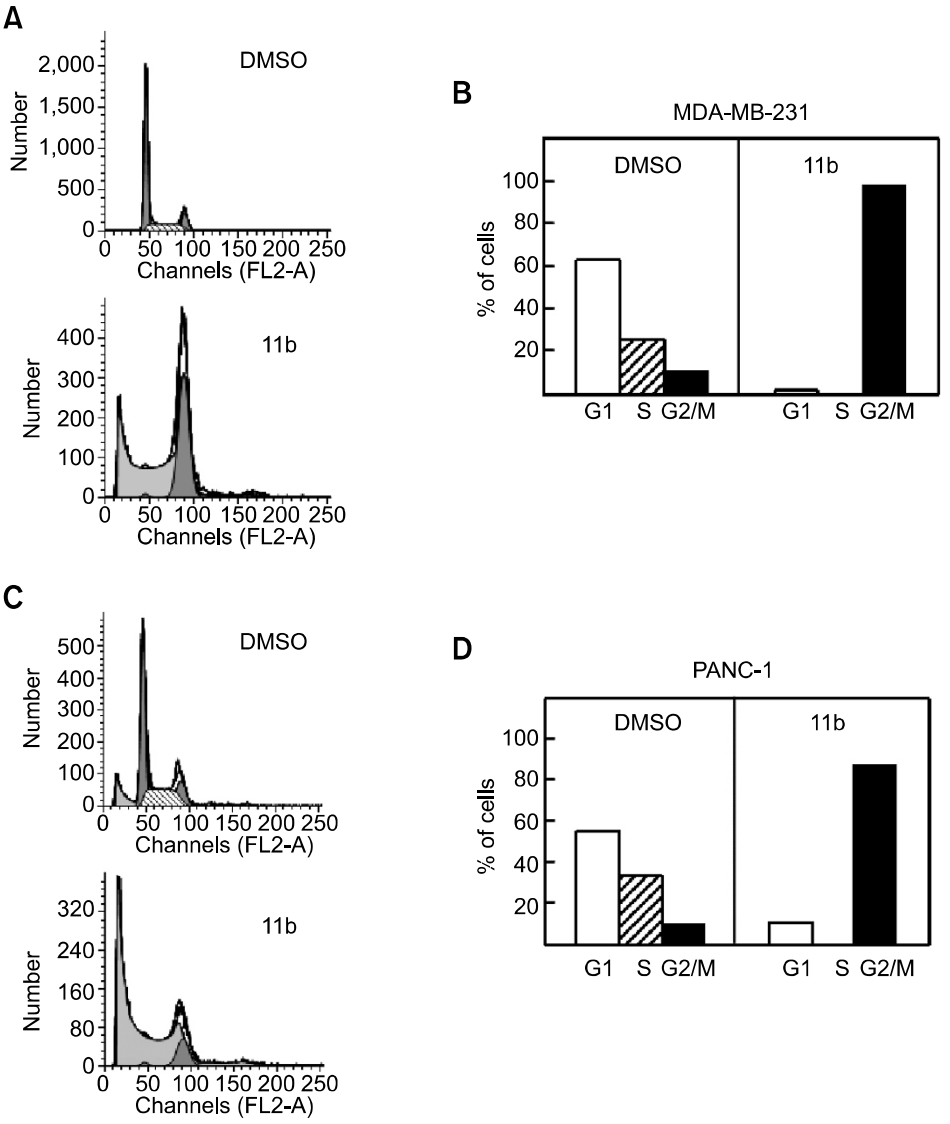


**Figure 3.** Flow cytometric analysis of MDA-MB-231 and PANC-1 cells. Cells were treated with 10 μM 11b for 24 h and then stained with propidium iodide (PI). Cell cycle distributions of MDA-MB-231 (A) and PANC-1 cells (C) were analyzed using FACS and the proportion of stained cells in the G1, S and G2/M phases in MDA-MB-231 (B) and PANC-1 cells (D) were measured.

transition (Sanchez and Dynlacht, 2005). These protein level and protein phosphorylation effects, combined with the FACS cell cycle results, suggest the hypothesis that 11b treatments arrest proliferating MDA-MB-231 and PANC-1 cells in metaphase and that well-known cell cycle regulatory proteins are likely to be involved in this cell cycle arrest.

### 11b treatments inhibit microtubule polymerization

Since 11b treatment resulted in cell cycle arrest and increased mitotic checkpoint protein levels and/or phosphorylation, we tested whether these 11b treatments might also interfere with microtubule assembly as other chemotherapeutic agents (taxanes or vinca alkaloids). Microtubule assembly was measured by the change of absorbance at 340 nm during 40 min reactions at 37°C. Severely reduced *in vitro* microtubule polymerization was observed with both 10 and 50 μM of 11b (Figure 5). In the absence of 11b, absorbance reached a plateau of OD 0.232 at 14 min. In contrast, 11b treatment slowed both the rates of increase in OD and the maximum ODs obtained, 0.083 for 10 μM of 11b and 0.036 for 50 μM of 11b after 40 min. Incubation with nocodazole, a well-characterized microtubule inhibitor, also reduced both the reaction rate and maximum OD (0.075).

We also observed severe alterations of the mitotic microtubule network in PANC-1 and MCF-7 cells treated with 11b. Control cells, without any treatments, exhibited the network staining pattern of normal microtubules (Figure 6A and G). Paclitaxel (1 μM), a tubulin stabilizing agent, promoted the formation of large microtubule bundles (Figure 6B

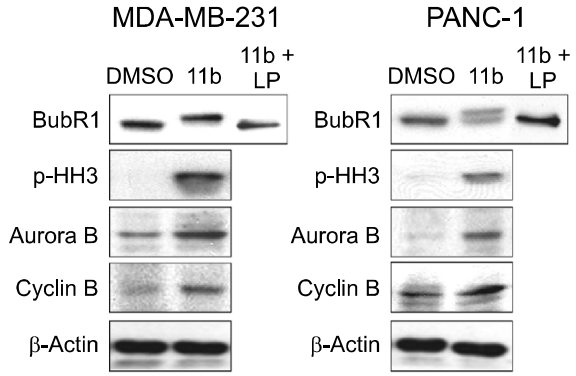


**Figure 4.** Effects of 11b on G2/M transition-related proteins. MDA-MB-231 and PANC-1 cells were incubated with or without 5 μM 11b for 24 h. Western blots were performed with anti-BubR1, anti-phospho-histone H3, anti-Aurora B and anti-cyclin B antibodies. Lambda phosphatase (LP, 100 units) was used for dephosphorylation of BubR1.

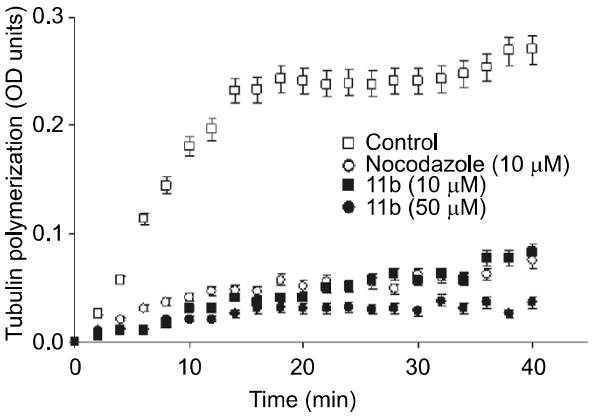


**Figure 5.** Inhibition of tubulin polymerization. *In vitro* tubulin polymerization assays were performed for 40 min at 37°C in the presence of 0.5% DMSO (the negative control), 10 μM nocodazole (the positive control), and 5 μM or 10 μM 11b. The kinetics and extent of tubulin polymerization was monitored by measuring optical density at 340 nM every two minutes. Data are means ± SE from three independent experiments.

and H), while nocodazole (10 μM), a tubulin depolymerzing agent, decreased microtubule amounts and/or density (Figure 6C and I). As expected from our *in vitro* microtubule polymerization experiments, treating cells for 3 h with either 5 μM 11b (Figure 6E and K) or 25 μM of 11b (Figure 6F and L) disrupted the microtubule network and decreased microtubule density. Incubation with 25 μM of resveratrol did not detectably alter the microtubule network of either the breast cancer or the pancreatic cancer cell lines (Figure 6D and J).

### Simulated docking of 11b into the colchicine binding site of tubulin

Molecular modeling studies, with docking simulations, were conducted to explore the interaction of 11b with tubulin. Docking simulations were produced using several potential binding conformations of 11b. All low-energy conformations of 11b were compared with the bound conformation of DMA-colchicine as determined from the crystal structure (PDB: 1SA0). The docking procedure was further validated by comparing the binding mode obtained by docking known tubulin polymerization inhibitors, including DMA-colchicine, podophyllotoxin, and combretastatin A-4. The results were quantified in terms of both lowest estimated energy of binding and RMSD between the binding conformation predicted by our model and others reported previously (Bai *et al*., 1996; Nogales *et al*., 1998; Ravelli *et al*., 2004; Kong *et al*., 2005; Lawrence and McGown, 2005). In this docking simulation, we found that the dimethoxyphenyl moiety of 11b was positioned similarly to that of the trimethoxyphenyl group of DMA-colchicine with an RMSD deviation of 0.71Å. This molecular conformation of 11b was chosen as an initial binding conformation for further molecular dynamics simulations.

Docking of inhibitors in a rigid protein binding site derived from a complex with another ligand may not predict correct binding mode due to the induced fit effect. Hence we further refined the binding mode of 11b using MD simulations. Initially, tubulin-11b complex was subjected to energy minimization to relieve any bad contacts. The minimized structure was then used for a MD simulation run of 200 ps, performed in the NVE ensemble. Since α,β-tubulin heterodimer is large, during the simulation, residues within 15Å of the ligand were allowed to move, whereas all other residues were kept fixed. Low-energy minimum structures were collected every 10 ps, giving a total of 20 structures and these are used for analysis. To evaluate the readjustment of the active site residues in the calculated tubulin-11b complexes, the RMSD between starting tubulin-11b complex and simulated tubulin-11b complex was determined. In the case of backbone atoms superimposition, the RMSD was lower than 0.4Å, whereas for side chains, the maximum RMSD found was approximately 0.95Å. These data show that ligand-induced conformational changes were minimal and more pronounced for side chains than for the polypeptide backbone.

Finally, the global energy minimum of the 20 low energy minimum structures was selected as the preferred binding model. As seen Figure 7, the three-dimensional arrangement of the dimethoxyphenyl moiety of 11b occupies the space similar to that of the trimethoxyphenyl group of the bound DMA-colchicine. This overlapping ensemble was

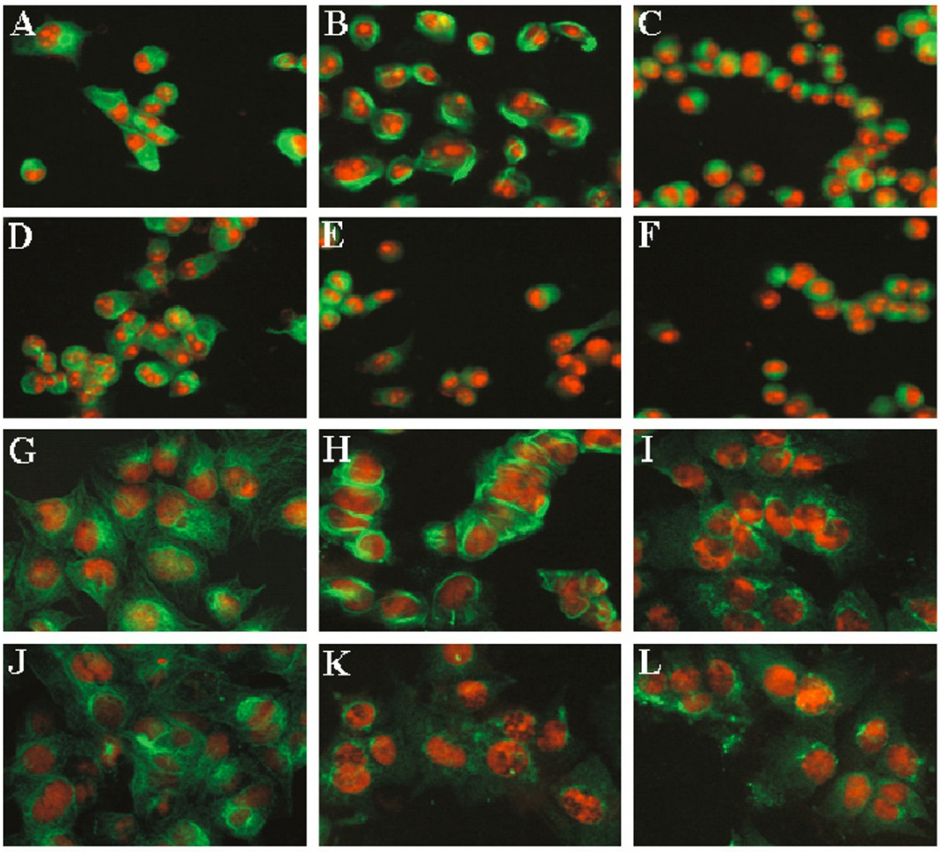


**Figure 6.** Immunofluorescent staining of microtubules in PANC-1 (A-F) and MCF-7 (G-L) cells. Cells treated for 3 h with 0.5% DMSO (A and G), 1 μM paclitaxel (B and H), 10 μM nocodazole (C and I), 25 μM resveratrol (D and J), 5 μM 11b (E and K), and 25 μM 11b (F and L), were stained with a β-tubulin antibody (green) and propidium iodide (red).

buried in the α,β-tubulin structure near the Leuβ238, Leuβ242, and Valβ318 (Figure 7). Analyses of 20 lowest-energy minima of 11b-tubulin complex revealed a potential H-bond interaction with Val-α181 as opposed to the starting complex structure. This corroborates the induced fit effect upon ligand binding to the tubulin and also suggests that, although ligand-induced conformational changes are minimal, such changes can be critical to the protein active site side chains during ligand binding. The molecular elements of the ligand connected to dimethoxyphenyl group of 11b were positioned in a slightly different location in the binding site than the molecular elements of DMA-colchicine relative to the trimethoxyphenyl group due to the non-planar nature of 11b. The dimethoxyphenyl moiety was buried well inside the hydrophobic pocket containing Val-β238, Cys-β241, Leu-β242, Leu-β248, Leu-β255, and Val-β318. Dimethoxy group of this moiety is oriented in such a way to form favorable hydrophobic interactions with the hydrophobic side chains of β-tubulin located above and below the plane of the phenyl ring.

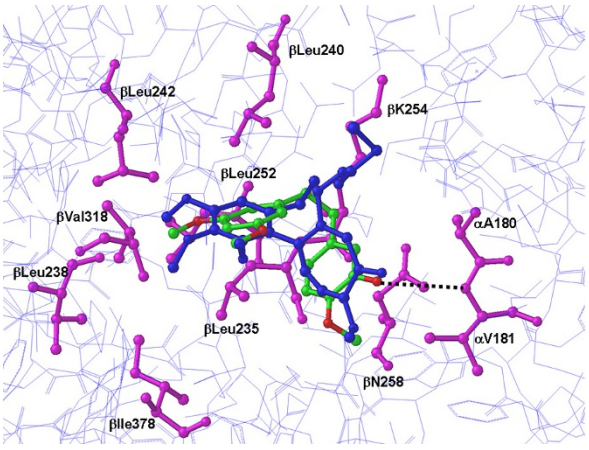


**Figure 7.** Molecular modeling of interaction of 11b with tubulin. The image shows overlayered binding models of both 11b and colchicine with α,β-tubulin. The polypeptide backbone of α,β-tubulin is rendered as a wire model (light blue). The interactive residue side chains of α,β-tubulin that bind colchicine at the colchicine site are colored magenta in stick rendering. The 11b and colchicine atoms are also shown in stick rendering, with the carbon atoms of bound colchicine colored blue. The oxygen atoms of 11b are colored red and the carbon atoms of 11b are colored green. The black broken line identifies one potential intermolecular hydrogen bond between 11b and α,β-tubulin.

## Discussion

According to Roverti *et al*. (2003), 11b is more cytotoxic than resveratrol for HL60 premyelocytic leukemia cells. The anti-proliferative activity ($IC_{50}$) and apoptotic-inducing activity ($AC_{50}$) of resveratrol towards HL60 cells was $5 \pm 0.9$ μM and $50 \pm 8.2$ μM, respectively. In contrast, the $IC_{50}$ and $AC_{50}$ values of 11b were at least 10-fold lower, $0.3 \pm 0.001$ μM for $IC_{50}$ and $0.04 \pm 0.0045$ μM for the $AC_{50}$ value (Roverti *et al*., 2003). Here, using cell lines derived from two other types of cancers, we found that resveratrol also had significantly less cytotoxic activity than 11b.

This study is the first to report that 11b is superior to resveratrol for killing and/or inhibiting the growth of breast and pancreatic cancer cell lines. These effects of 11b are likely to be related to the ability of 11b to disrupt microtubule polymerization *in vitro*. Simulations of the molecular docking between α,β-tubulin and either colchicine or 11b suggest that the dimethoxyphenyl group of 11b could occupy almost exactly the same space as the trimethoxyphenyl group of colchicine. In addition, since the hydroxyl group of 11b could potentially form an H-bond with Val-α181 of tubulin (Figure 7), our simulations suggest a mechanistic explanation for the greater potency of 11b (i.e., resveratrol does not form H-bonds in our binding pocket simulations). In our simulation 11b is buried in the hydrophobic cavity created by three tubulin residues, Leuβ238, Leuβ242, and Valβ318 (Figure 7). Ensembles of 11b revealed H-bond interaction with Val-α181 due to the induced fit effect upon ligand binding, which suggests that ligand-induced conformational changes can be critical to the protein active site side chains during ligand binding. Thus, the dimethoxyphenyl moiety buried deep into the hydrophobic pocket can make interactions with β-tubulin similar to the interactions identified for the trimethoxyphenyl moiety of DMA-colchicine.

Our results also suggest that the molecular level effects of 11b described here, binding to tubulin, inducing changes in the tubulin structure and increasing the expression and/or phosphorylation of mitosis checkpoint protein such as BubR1, p-HH3, Aurora B, and Cyclin B, may at least partially explain the biological effects of 11b on breast and pancreatic cancer cells. That is, it has been previously shown that defects in microtubule polymerization prevent microtubules from attaching to centromeres during metaphase (Weaver and Cleveland, 2005) and that the absence of normal centromere-microtubule interactions activates mitotic checkpoint proteins, resulting in a block of cell cycle progression into anaphase and failure to form anaphase-promoting complex (Weaver and Cleveland, 2005). Although our data does not allow us to decide which of the biochemical effects of 11b described here, blocking microtubule polymerization or inducing/activating cell cycle checkpoint proteins, is the primary effect, numerous studies suggest that blocking microtubule polymerization activates cell cycle checkpoints (reviewed in Cuschieri *et al*., 2007).

The results of our study are also consistent published studies suggesting that apoptosis pathways can be activated by treatments with agents that block microtubule polymerization (Ikegami *et al*., 1997; Gorman *et al*., 1999). Our studies found that treatments with low concentrations of 11b caused 98% (MDA-MB-231) and 88% (PANC-1) of live cells (excluding sub-G0/G1 fraction) to accumulate at the G2/M transition. Long-term arrest of cells in the M phase is known to drive cells to apoptotic cell death mediated by Bax, PARP, and caspase-3 (Tao *et al*., 2005). In this study, we found that 11b treatments caused 57% (MDA-MB-231) and 86% (PANC-1) of total cells to accumulate at a position of hypoploid fraction, indicative of apoptosis, in a standard FACS analysis. However, our study does not provide direct evidence that the increased cells in sub-G0/G1 fractions are apoptotic cells.

In these studies, we showed that 11b has greater activity than resveratrol for blocking microtubule polymerization *in vitro*, for blocking *in vivo* cell proliferation and for promoting cell death. Further study of the effects of and mechanism(s) involved in 11b-caused cytotoxicity, especially in appropriate animal models are warranted to determine if this resveratrol derivative may have potential in humans, either as a chemopreventive agent for pancreatic cancer or as an anti-tumor agent for breast cancer.

## Methods

### Cell culture

Human pancreatic cancer cell lines were cultured in either DMEM (PANC-1) or RPMI 1640 media (AsPC-1 and Colo-357) supplemented with 10% FBS. Human breast cancer cell lines, MCF-7 and MDA- MB231, were cultured in DMEM supplemented with 5% FBS. All cell culture reagents were purchased from BioWhittaker, Inc. (Walkersville, MD).

### Cell viability assay

Cell survival was determined by MTT assays as previously described (Bae *et al*., 2004). Cells were seeded in 96-well plates at densities of $3 \times 10^4$ cells per well, grown overnight, treated with different concentrations of 11b or resveratrol for 24 h and then assayed for MTT dye

reduction. Cell viability values were calculated as a percentage of the control cells (100%) and expressed as means ± SE for three independent experiments.

### Cell cycle analysis

MDA-MB-231 and PANC-1 cells were cultured with or without 10 μM of 11b for 24 h, detached with trypsin/EDTA buffer, harvested, washed with cold PBS, and fixed with 70% ethanol for 30 min at 4°C. The fixed cells were treated with DNA staining solution (3.4 mM Tris-Cl (pH 7.4), propodium iodide, 0.1% triton X-100 buffer and 100 μg/ml RNase A). These samples were then analyzed with FACSort (Becton Dickson, San Jose, CA) at the Flow Cytometry and Cell Sorting Core Facility of Georgetown University Medical School. Cell cycle distributions were determined using Modfit software (Verity Softwarehouse, Topsham, ME). At least 20,000 events were collected and analyzed for each measurement, as previously described (Bae *et al*., 2005).

### Western blot analysis

MDA-MB-231 and PANC-1 cells were cultured with or without 5 μM of 11b for 24 h, and lysed in a buffer (50 mM Tris-Cl, pH 8.0, 150 mM NaCl, 1% Nonidet P-40). The proteins in total cell extracts were separated on SDS-PAGE gels, Western blots were prepared as described in Kim *et al*. (2006) and then analyzed using anti-BubR1 mouse monoclonal antibody (BD Bioscience Inc., Bedford, MA), anti-phospho-histone H3 (Cell Signaling Technology, Inc., Boston, MA), anti-Aurora B, anti-Cyclin B (Abcam, Inc., Cambridge, MA) and anti-β actin (Santa Cruz Biotechnology Inc., Santa Cruz, CA) as the primary antibodies. The membranes were then incubated for 1 h at room temperature with HRP-conjugated secondary antibodies. Membrane bound secondary antibodies were visualized by enhanced chemiluminescence (ECL) (Santa Cruz Biotechnology) detection kits.

### Tubulin polymerization assay

Tubulin polymerization was analyzed with a tubulin polymerization assay kit from Cytoskeleton, Inc. (Denver, CO). Assays were performed according to the manufacturer's protocol. Reaction mixtures containing 10 mg/ml of tubulin in the presence of 10 μM nocodazole and 10 μM or 50 μM 11b were placed in quartz cuvettes and incubated at 37°C. The turbidity resulting from the polymerized tubulin was measured every two minutes as absorbance at 340 nm, using an ultra 384 spectrophotomer (Tecan, Research Triangle Park, NC) at the Macromolecular Analysis Core Facility of Georgetown University Medical School.

### Immunofluorescence staining

PANC-1 cells, cultured on poly-D-lysine coated coverslips (BD Bioscience, Bedford, MA), were incubated for 3 h with or without 10 μM nocodazole and either 10 μM or 50 μM of 11b. Cells were then washed with PBS, fixed with 4% paraformaldehyde for 15 min, and permeabilized with 0.5% Triton X -100 for 5 min. Cells were then incubated with monoclonal anti β-tubulin antibody (Sigma, St. Louis, MO) for 1 h, washed in PBS, and incubated with Alexa-fluor 488 conjugated goat anti-mouse IgG (Molecular Probes, Eugene, OR) and propidium iodide. Fluorescence images were taken with a fluorescence microscope (Olympus).

### Molecular modeling and docking simulations

The X-ray crystal structure of α,β-tubulin heterodimers complexed with DMA-colchicine and a stathmin fragment (PDB: 1SA0) was used for the molecular docking of the compound 11b. Inconsistencies between the PDB format and the tubulin residues library translation to atomic potential types were corrected manually. First, the 11b ligand was constructed using SYBYL8.0 (Tripos, Inc., St. Louis, MO) and optimized with MP2/6-31G* basis set using the Gaussian 03 quantum mechanical program (Frisch *et al*., 2003). Docking experiments were performed with the FlexX program (Rarey *et al*., 1996). In FlexX, all the parameters were used in their default settings, except that the number of solution conformations was set to 90. The best docked geometry for 11b was minimized using AMBER9.0 (Case *et al*., 2006). The minimized complex was subjected to 200ps molecular dynamics (MD) simulations to relax the protein-inhibitor complex. MD simulations were carried out using the SANDER module of the AMBER9.0 simulation package (Case *et al*., 2006) with the PARM98 force-field parameter. The SHAKE algorithm (Hanson *et al*., 2003) was used to keep all bonds involving hydrogen atoms rigid. Weak coupling temperature and pressure coupling algorithms (Berendsen *et al*., 1984) were used to maintain constant temperature and pressure, respectively. MD simulations were performed using 0.001 picosecond (ps) time steps with temperature set at 300 K. Electrostatic interactions were calculated with the Ewald particle mesh method (Darden *et al*., 1993) with a dielectric constant at $1R_{ij}$ and a nonbonded cutoff of 12 Å for the real part of electrostatic interactions and for van der Waals' interactions.

### Acknowledgements

Dr. Bae has been supported by the National Institute of Environmental Health Science, NIH (ES01440-01), U. S. Department of Defense (DOD) Breast Cancer Program Idea Award (DAMD17-02-1-0525), American Cancer Society (IRG 97-152-13), and Susan G. Komen for the Cure (BCTR119906 and FAS0703858). Dr. Rosen has been supported by the USPHS Grant (R01-CA104546). We appreciate Dr. Thomas L. Mattson for helpful discussions and editing.

## References

Adams RR, Carmena M, Earnshaw WC. Chromosomal passengers and the aurora ABCs of mitosis. Trends Cell Biol 2001;11:49-54

Athar M, Back JH, Tang X, Kim KH, Kopelovich L, Bickers DR, Kim AL. Resveratrol: a review of pre-clinical studies for

human cancer prevention. Toxicol Appl Pharmacol 2007; 224:274-83

Azios NG, Krishnamoorthy L, Harris M, Cubano LA, Cammer M, Dharmawardhane SF. Estrogen and resveratrol regulate Rac and Cdc42 signaling to the actin cytoskeleton of metastatic breast cancer cells. Neoplasia 2007;9:147-58

Bae I, Fan S, Meng Q, Rih JK, Kim HJ, Kang HJ, Xu J, Goldberg ID, Jaiswal AK, Rosen EM. BRCA1 induces antioxidant gene expression and resistance to oxidative stress. Cancer Res 2004;64:7893-909

Bae I, Rih JK, Kim HJ, Kang HJ, Haddad B, Kirilyuk A, Fan S, Avantaggiati ML, Rosen EM. BRCA1 regulates gene expression for orderly mitotic progression. Cell Cycle 2005; 11:1641-66

Bai R, Pei XF, Boye O, Getahun Z, Grover S, Bekisz J, Nguyen NY, Brossi A, Hamel E. Identification of cysteine 354 of β-tubulin as part of the binding site for the A ring of colchicine. J Biol Chem 1996;271:12639-45

Berendsen HJC, Postma JPM, Vangunsteren WF, Dinola A, Haak AR. Molecular-dynamics with coupling to an external bath. J Chem Phys 1984;81:3684-90

Buzdar AU. Preoperative Chemotherapy Treatment of Breast Cancer-A Review. Cancer 2007;110:2394-407

Case DA, Darden TA, Cheatham TE, Simmerling CL, Wang J, Duke RE, Luo R, Merz KM, Pearlman DA, Crowley M, Walker RC, Zhang W, Wang B, Hayik S, Roitberg A, Seabra G, Wong KF, Paesani F, Wu X, Brozell S, Tsui V, Gohlke H, Yang L, Tan C, Mongan J, Hornak V, Cui G, Beroza P, Mathews DH, Schafmeister C, Ross WS, Kollman PA, AMBER 9, 2006, University of California, San Francisco.

Chen RH. BubR1 is essential for kinetochore localization of other spindle checkpoint proteins and its phosphorylation requires Mad1. J Cell Biol 2002;158:487-96

Cuschieri L, Nguyen T, Vogel J. Control at the cell center: the role of spindle poles in cytoskeletal organization and cell cycle regulation. Cell Cycle 2007;6:2788-94

Darden T, York D, Pedersen L. Particle mesh Ewald: an N.Log(N) method for Ewald sums in large systems. J Chem Phys 1993;98:10089-92

Ding XZ, Adrian TE. Resveratrol inhibits proliferation and induces apoptosis in human pancreatic cancer cells. Pancreas 2002;25:71-6

Epelbaum R, Rosenblatt E, Nasrallah S, Faraggi D, Gaitini D, Mizrahi S, Kuten A. Phase II study of gemcitabine combined with radiation therapy in patients with localized, unresectable pancreatic cancer. J Surg Oncol 2002;81: 138-43

Frisch MJ, Trucks GW, Schlegel HB, Scuseria GE, Robb MA, Cheeseman JR, Montgomery JA Jr, Vreven T, Kudin KN, Burant JC. Gaussian 03, 2003, Gaussian, Inc., Pittsburgh, PA.

Gorman AM, Bonfoco E, Zhivotovsky B, Orrenius S, Ceccatelli S. Cytochrome c release and caspase-3 activation during colchicine-induced apoptosis of cerebellar granule cells. Eur J Neurosci 1999;11:1067-72

Hanson RN, Lee CY, Friel CJ, Dilis R, Hughes A, DeSombre ER. Synthesis and evaluation of 17α-20E-21-(4-substituted phenyl)-19-norpregna-1,3,5(10),20-tetraene-3,17β-diols as probes for the estrogen receptor hormone binding domain. J Med Chem 2003;46:2865-76

Ikegami R, Zhang J, Rivera-Bennetts AK, Yager TD. Activation of the metaphase checkpoint and an apoptosis programme in the early zebrafish embryo, by treatment with the spindle-destabilising agent nocodazole. Zygote 1997;5: 329-50

Ishii H, Okada S, Tokuuye K, Nose H, Okusaka T, Yoshimori M, Nagahama H, Sumi M, Kagami Y, Ikeda H. Protracted 5-fluorouracil infusion with concurrent radiotherapy as a treatment for locally advanced pancreatic carcinoma. Cancer 1997;79:1516-20

Jang M, Cai L, Udeani GO, Slowing KV, Thomas CF, Beecher CWW, Fong HHS, Farnsworth NR, Kinghorn AD, Menta RG, Moon RC, Pezzuto JM. Cancer chemopreventive activity of resveratrol, a natural product derived from grapes. Science 1997;275:218-20

Jimeno A, Hidalgo M. Molecular biomarkers: their increasing role in the diagnosis, characterization, and therapy guidance in pancreatic cancer. Mol Cancer Ther 2006;5:787-96

Kim EY, Hong YB, Go SH, Lee B, Jung SC. Downregulation of neurotrophic factors in the brain of a mouse model of Gaucher disease; implications for neuronal loss in Gaucher disease. Exp Mol Med 2006;38:348-56

Kim R, Saif MW. Is there an Optimal Neoadjuvant Therapy for Locally Advanced Pancreatic Cancer? J Pancreas 2007; 8:279-88

Kong Y, Grembecka J, Edler MC, Hamel E, Mooberry SL, Sabat M, Rieger J, Brown ML. Structure-based discovery of a boronic acid bioisostere of combretastatin A-4. Chem Biol 2005;12:1007-14

Kuroiwa Y, Nishikawa A, Kitamura Y, Kanki K, Ishii Y, Umemura T, Hirose M. Protective effects of benzyl isothiocyanate and sulforaphane but not resveratrol against initiation of pancreatic carcinogenesis in hamsters. Cancer Lett 2006;241:275-80

Lawrence NJ, McGown AT. The chemistry and biology of antimitotic chalcones and related enone systems. Curr Pharm Des 2005;11:1679-93

Le Corre L, Chalabi N, Delort L, Bignon YJ, Bernard-Gallon DJ. Resveratrol and breast cancer chemoprevention: molecular mechanism. Mol Nutr Food Res 2005;49:462-71

Lockhart AC, Rothenberg ML, Berlin JD. Treatment for pancreatic cancer: current therapy and continued progress. Gastroenterology 2005;128:1642-54

Nogales E, Wolf SG, Downing KH. Structure of the alpha beta tubulin dimer by electron crystallography. Nature 1998;391: 199-203

Ota T, Suto S, Katayama H, Han ZB, Suzuki F, Maeda M, Tanino M, Terada Y, Tatsuka M. Increased mitotic phosphorylation of histone H3 attributable to AIM-1/Aurora-B overexpression contributes to chromosome number instability. Cancer Res 2002;62:5168-77

Provinciali M, Re F, Donnini A, Orlando F, Bartozzi B, Di Stasio G, Smorlesi A. Effect of resveratrol on the development of spontaneous mammary tumors in HER-2/neu transgenic mice. Int J Cancer 2005;115:36-45

Rarey M, Kramer B, Lengauer T, Klebe G. A fast flexible docking method using an incremental construction algorithm. J Mol Biol 1996;261:470-89

Ravelli RB, Gigant B, Curmi PA, Jourdain I, Lachkar S, Sobel A, Knossow M. Insight into tubulin regulation from a complex with colchicine and a stathmin-like domain. Nature 2004; 428:198-202

Rich T, Harris J, Abrams R, Erickson B, Doherty M, Paradelo J, Small W Jr, Safran H, Wanebo HJ. Phase II study of external irradiation and weekly paclitaxel for nonmetastatic, unresectable pancreatic cancer: RTOG-98-12. Am J Clin Oncol 2004;27:51-6

Roberti M, Pizzirani D, Simoni D, Rondanin R, Baruchello R, Bonora C, Buscemi F, Grimaudo S, Tolomeo M. Synthesis and Biological Evaluation of Resveratrol and Analogues as Apoptosis-Inducing Agents. J Med Chem 2003;46:3546-54

Sanchez I, Dynlacht BD. New insights into cyclins, CDKs, and cell cycle control. Semin Cell Dev Biol 2005;16:311-21

Tao W, South VJ, Zhang Y, Davide JP, Farrell L, Kohl NE, Sepp-Lorenzino L, Lobell RB. Induction of apoptosis by an inhibitor of the mitotic kinesin KSP requires both activation of the spindle assembly ckeckpoint and mitotic slippage. Cancer Cell 2005;8:49-59

Weaver BAA, Cleveland DW. Decoding the links between mitosis, cancer, and chemotherapy: the mitotic checkpoint, adaptation, and cell death. Cancer Cell 2005;8:7-12

Wei Y, Yu L, Bowen J, Gorovsky MA, Allis CD. Phosphorylation of histone H3 is required for proper chromosome condensation and segregation. Cell 1999;97:99-109